American Mineralogist, Volume 84, pages 1569–1576, 1999

Vibrational spectroscopic study of minerals in the Martian meteorite ALH84001

T.F. COONEY,[1,*] E.R.D. SCOTT,[1] A.N. KROT,[1] S.K. SHARMA,[1,†] AND A. YAMAGUCHI[2]

[1]Hawaii Institute of Geophysics and Planetology, University of Hawaii, Honolulu, Hawaii 96822, U.S.A.
[2]National Institute for Research in Inorganic Materials 1-1 Namiki, Tsukuba 305, Japan

ABSTRACT

Micro-Raman spectra of carbonates, silica and amorphous plagioclase, and both micro-Raman and IR reflectance spectra of phosphates in ALH84001 are reported. Data from these vibrational techniques combined with electron microprobe analyses show that (1) the carbonates exhibit complex compositional heterogeneity on a sub-micrometer scale, (2) the phosphates, chlorapatite and merrillite, are largely anhydrous, (3) amorphous silica and plagioclase experienced peak shock pressures >32 GPa and >50 GPa, respectively, and (4) vitreous plagioclase was quenched from a shock-induced melt after relaxation of the peak shock pressure. The observed general Raman band broadening of lattice and internal modes of carbonates in ALH84001 indicates complex sub-microscopic compositional heterogeneity and possibly structural disorder. Any search for biogenic markers in ALH84001 must recognize the complex shock and thermal history of these minerals.

INTRODUCTION

The claim of possible evidence of ancient life in the carbonate globules of the Martian meteorite ALH84001 (McKay et al. 1996) has intensified controversy over the origin of these carbonates. Proposed alternatives to biogenic formation include high-temperature hydrothermal (Mittlefehldt 1994; Harvey and McSween 1996); vapor-phase (Bradley et al. 1996) precipitation, low-temperature fluid-mediated precipitation (Romanek et al. 1994; Valley et al. 1997); replacement of maskelynite (Gleason et al. 1997; Kring et al. 1998); or shock melting of preexisting carbonates (Scott et al. 1997). Studies of the chemical and isotopic compositions of the carbonates (Harvey and McSween 1996; Romanek et al. 1994; Valley et al. 1997; Treiman 1997; Leshin et al. 1998; Saxton et al. 1998) have failed to develop convincing constraints on their formation temperatures. Also, there is little agreement on pressures and geological processes that affected the carbonates and associated interstitial phases: silica, vitreous plagioclase, and phosphates. Although chemical (Mittlefehldt 1994; Harvey and McSween 1996; Gleason et al. 1997; Scott et al. 1997) and isotopic (Romanek et al. 1994; Valley et al. 1997) zoning in the carbonates are well characterized, the degree of structural disorder is not known.

Petrographic and structural studies on other accessory phases in ALH84001 can provide additional constraints on the petrogenetic history of the rock. Silica, which is a sensitive indicator of the degree of shock metamorphism (Stöffler and Langenhorst 1994), occurs as a scattered accessory phase in ALH84001, although its structure has not yet been identified. Phosphates are important interstitial trace minerals in ALH84001 (Mittlefehldt 1994) and other Martian meteorites because they might contain significant amounts of water (Leshin et al. 1996). Plagioclase-composition regions in ALH84001, although presumably initially crystalline feldspar, have attained their current amorphous character either by melting or by solid state amorphization. Correct interpretation of the geochemical and petrographic data requires mineralogical and structural information for these minor phases. Vibrational techniques, including infrared (IR) and micro-Raman (e.g., Sharma 1989; Wopenka et al. 1996; El Gorsey 1997) spectroscopy, can give information on the structures of these minerals thereby providing constraints on phase identification, peak shock pressure, and possible sub-microscopic exsolution. This study reports confocal micro-Raman spectroscopy directly on mineral grains in polished thin sections of the meteorite ALH84001.

EXPERIMENTAL PROCEDURES

Samples

Detailed chemical analyses of ALH84001 carbonates in the literature (Mittlefehldt 1994; Harvey and McSween 1996; Gleason et al. 1997; Scott et al. 1997; Kring et al. 1998) indicate a zoning trend from ferroan dolomite to nearly pure magnesite with an abrupt compositional gap between the inner zoned core and the outer magnesite mantle. Figure 1 is a backscattered electron image of a representative irregular carbonate patch showing the locations of Raman microprobe analyses of the mantle and core regions ("1" and "2", respectively, in Fig. 1). These spots are located on either side of the inner ring of opaque inclusions (thin bright strips in Fig. 1)

*Current address: Avanex Corporation, 42501 Albrae Street, Fremont, California 94538, U.S.A.
†E-mail: sksharma@soest.hawaii.edu

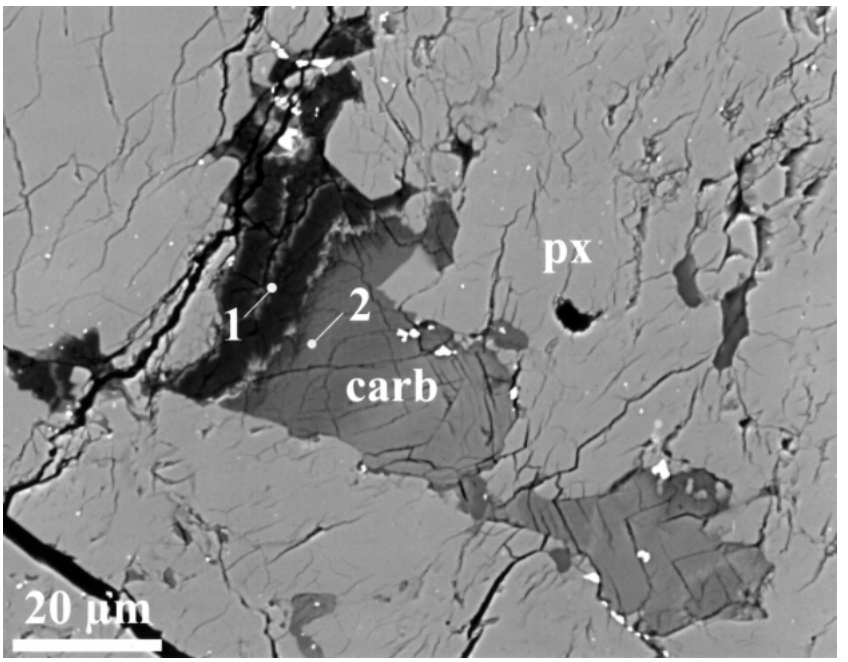

FIGURE 1. Backscattered electron image of chemically zoned carbonate (labeled, "carb") in orthopyroxene (px) in ALH84001,6 showing location of micro-Raman analyses (points marked as 1 and 2).

demarcating the compositional gap between the magnesite mantle and more calcic core. Figure 2 presents backscattered electron images of the silica grain and intergrown phosphate phases examined here. Electron microprobe analyses are in Table 1. Analyses with a rastered electron probe beam show that most feldspathic grains have plagioclase stoichiometry around $An_{30–37}$,$Or_{3–5}$ (Table 1; Mittlefehldt 1994; Scott et al. 1997).

Based upon the microprobe analyses, the phosphate mineral designated "Cl-apt" in Figure 2b is identified as chlorapatite. Based upon the same set of electron microprobe analyses, as well as Raman, and IR spectroscopy (see below), the phosphate mineral designated "merr" is identified as merrillite. This phase, which was previously misnamed "apatite" (Mittlefehldt 1994), is commonly called "whitlockite" (e.g., Boctor et al. 1998). However, Dowty (1977) has shown that whitlockite and merrillite are structurally distinct minerals and that the name whitlockite should only be used for the hydrous mineral, which occurs on Earth but is absent in lunar rocks and chondrites. We follow Dowty's suggestion (Dowty 1977) as the IMA Commission on New Minerals and Mineral Names (Rubin 1997) approved it. Microprobe reconnaissance suggests that merrillite is more abundant than apatite in ALH84001.

Raman spectra

All results reported herein were obtained from minor minerals located within pyroxene inter-grain boundaries in ALH84001,6 and ALH84001,146. Confocal micro-Raman and Fourier-Transform IR reflectance spectra were obtained from carbonates, phosphates, silica, and amorphous plagioclase. Only a single hemispherical silica grain was found that was large enough for Raman analysis. Mineral compositions were analyzed with a Cameca Camebax electron probe analyzer at 15 keV using a beam current of 5–10 nA, well-analyzed standards, and a ZAF correction procedure. Reference Raman spectra of the microscope slide and mounting epoxy in each thin section were also recorded to guard against mis-identification of spectral peaks arising from thin section substrates.

The confocal micro-Raman system used here was described in detail by Sharma et al. (1996). Raman spectra were obtained from selected ~1 µm spots and with axial resolution of 2 µm using a modified Leitz Ortholux I petrographic microscope, coupled to a Spex Triplemate grating spectrometer outfitted with a multichannel photo-detector (either a Photometrics or Princeton Instruments liquid-nitrogen-cooled CCD). An internal moveable prism assembly at the top of the microscope was used to toggle the light path between the eyepiece and the spectrometer. All experiments were performed in 180° backscattering geometry using a 45° dichroic beam splitter housed midway within the microscope tube to direct part of the incident laser beam (Ar^+ 488.0 or 514.5 nm) vertically downward through the objective and onto the sample. The same 160X microscope objective with numerical aperture (N.A.) of 0.95 was used for both focusing the laser to a 1 µm diameter spot as well as for collecting Raman backscattered light from the sample. Most spectra were obtained using a 1200 grooves/mm grating with slits set for 4 cm^{-1} resolution, although a few spectra of the lattice mode region of carbonates were obtained using a 1800 grooves/mm grating and 3 cm^{-1} resolution. In these higher resolution spectra, it was not possible to measure simultaneously the strongest C-O stretching mode (near 1090 cm^{-1}) with the carbonate lattice modes because of high dispersion.

The simple confocal modification used in the Raman analysis of thin sections consisted of spatial and/or N.A. filters placed between the microscope and the spectrometer. The N.A. filter (i.e., *f*-stop) consisted of a set of mutually perpendicular slits

TABLE 1. Electron microprobe analysis (in weight percent) of minerals in ALH84001

	No. of analyses	SiO_2	Al_2O_3	Cr_2O_3	FeO	MnO	MgO	CaO	Na_2O	K_2O	Cl	P_2O_5	Total
Carbonate 1†	||	0.05	<0.02	0.1	1.1	0.1	45.4	2.6	0.1	<0.02	*	*	101.9**
Carbonate 2†	||	0.1	<0.02	0.1	22.6	0.3	25.8	4.8	0.2	<0.02	*	*	100.3**
Silica‡	7	97.3	0.03	<0.03	0.27	<0.02	<0.02	0.03	0.11	0.04	*	*	97.74#
Phosphate (merr)§	6	0.05	<0.03	<0.03	0.73	0.04	3.4	46.6	*	*	<0.03	45.7	96.52#
Phosphate (Cl-apt)§	2	0.22	<0.03	<0.03	0.18	0.03	0.04	53.7	*	*	4.4	40.9	99.47
Plagioclase Phase	||	59.9	25.3	0.1	0.4	<0.02	<0.02	6.8	7.3	0.62	*	*	100.42

* Not analyzed.
† Figure 1. These compositions were estimated based on analyses of several carbonate grains.
‡ Figure 2a.
§ Figure 2b.
|| Representative analysis of phases.
Low total probably due to use of a pyroxene standard for Si analyses.
** Sum includes CO_2 calculated assuming stoichiometry.

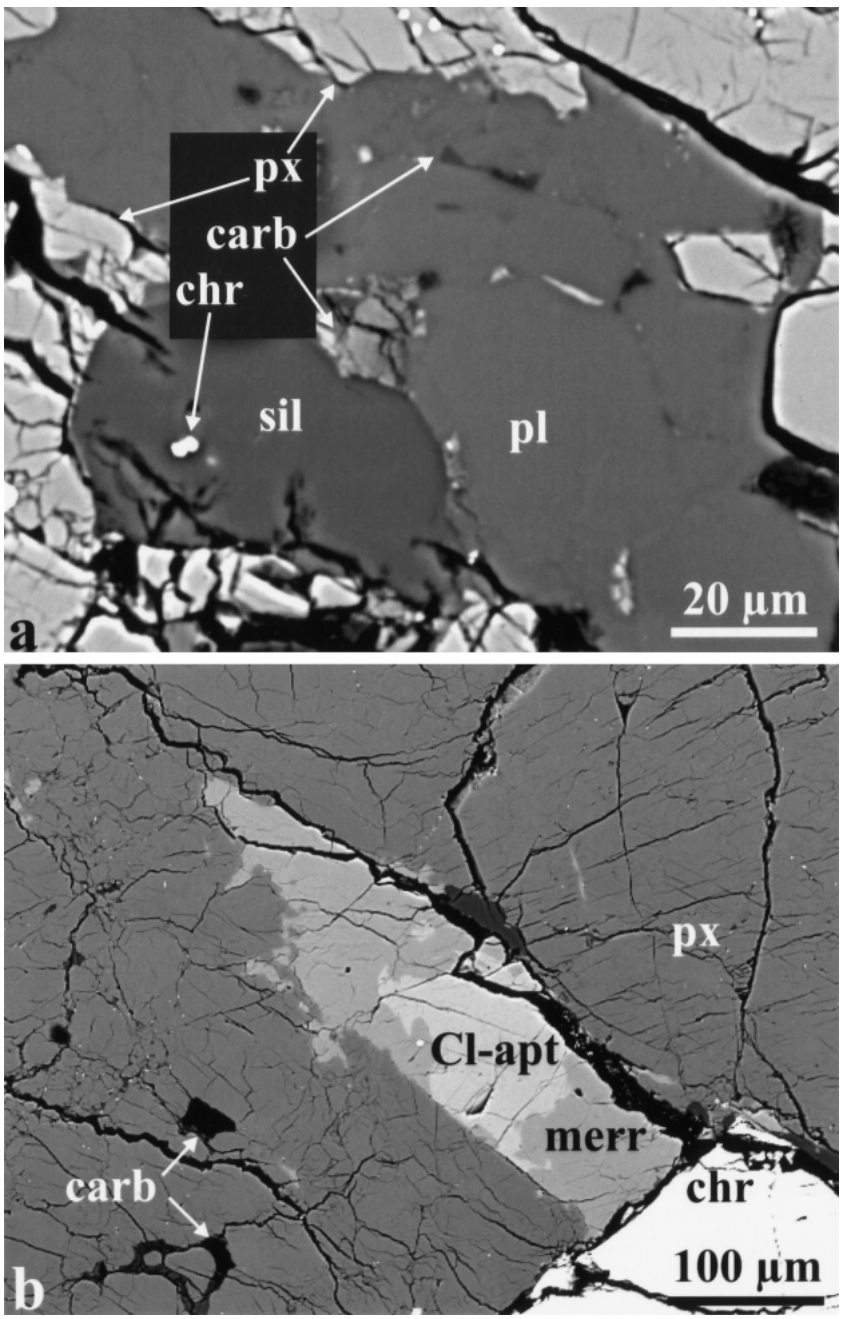

FIGURE 2. Backscattered electron images of minerals in ALH84001,6: (**a**). Hemispherical silica grain (labeled, "sil") associated with carbonate and plagioclase glass (pl) in an inter-grain boundary; and (**b**) Inter-grown phosphates, chloroapatite (labeled, "Cl-apt")and merrillite (labeled, "merr"), in an inter-grain boundary.

attached to the microscope. The spatial (confocal) filter consisted of two co-axial mutually facing microscope objectives and an intervening piece of metal foil with a 20 μm round pinhole. Collimated scattered light collected by the microscope was focused onto and through the pinhole by the first objective and re-collimated by the second objective.

Experimental trade-offs exist between spectral quality and spatial resolution in confocal micro-Raman analyses of petrographic thin sections. The small laser beam spot size (roughly 1 μm diameter with the 160× objective), necessary for lateral and depth spatial resolution, also gives rise to extremely high laser power densities at the sample (on the order of 3 MW/cm^2 for 30 mW total power). Unfortunately, Raman signal strength only depends on the total available laser power (i.e., not power density). The degree to which any given mineral grain can tolerate such power densities without damage depends upon its intrinsic properties—thermodynamic stability and optical absorbance—as well as the comparable properties of any included phases. Minerals grains particularly susceptible to laser damage include those that are strongly colored (such as the carbonates and pyroxenes of ALH84001), have sub-microscopic opaque or colored inclusions (such as ALH84001 carbonates), and those that are thermodynamically unstable (such as the high-pressure stishovite form of silica that could be present in shocked meteorites). Clear, inclusion-free minerals such as feldspars, feldspar glasses, and possibly phosphates present fewer problems because most of the beam energy is simply transmitted through the sample. As a compromise, variable laser power, approximately 30 mW for Raman analyses of vitreous plagioclase (ALH84001,146) and 4 mW or less for Raman analyses of carbonates, silica, and phosphates (ALH84001,6), was used such that acceptable spectra were obtained without producing visible beam damage.

In addition, the confocal modifications attenuate a significant proportion of the spectral intensity. The combined effects of low laser power (for some mineral grains), confocal optics, and small Raman scattering cross sections (for some phases, especially silicate glasses) results generally in low intensity. Furthermore, virtually unavoidable fluorescence from mounting epoxy (which has been subtracted from the presented spectra) adds a significant degree of "shot noise" but no usable "signal." Therefore, the signal-to-noise ratios in the spectra were enhanced by using long exposure times. Exposure times of approximately one hour were used for each of the spectra reported here. These conditions have produced adequate-quality spectra for most grains except, perhaps, for the single analyzed silica grain which had limited thickness and which was analyzed with low laser power.

Infrared reflectance spectra

Infrared reflectance spectra were obtained with a Spectra-Tech IR-Plan microscope interfaced to a Bomem DA3 FTIR spectrometer equipped with a KBr beam splitter and a liquid-nitrogen-cooled MCT detector. Analyses were obtained from circular 100 μm diameter regions on the sample by inserting a block with a 1 mm hole at the image plane (i.e., 10× magnification) at the top of the microscope. A gold foil standard was used for the reference spectra.

Results and discussion

Carbonates

The Raman bands shown in Figure 3 include two lattice modes (librational and translational) below 345 cm^{-1} and the ν_4 (O-C-O in-plane bending) mode of carbonate ion near 730 cm^{-1} (White 1974). Concurrently, the ν_1 Raman band corresponding to the C-O symmetric stretch mode (Fig. 4) ranges from near 1084 to near 1094 cm^{-1}. In accord with electron microprobe analyses (Table 1) the band positions in the Raman spectrum of the mantle region are similar to those of pure magnesite whereas those of the inner core regions are significantly broader and shifted toward lower wavenumbers than ferroan magnesite. The Raman bands of the meteoritic carbonates are, however, significantly broader than any of the terrestrial end-members (see e.g., Herman et al. 1987). Also, spectra obtained from the non-mantle carbonate regions often exhibit band asymmetry (e.g., 312 cm^{-1} band of Fig. 3) and partial splitting (Figs. 3 and 4), and they invariably display a broad band near 674 cm^{-1} and weaker bands near 368 and 410 cm^{-1}. These latter three bands probably arise from magnetite (Wang et al. 1998), which is known to occur as scattered sub-microscopic inclusions in this sample (McKay et al. 1996).

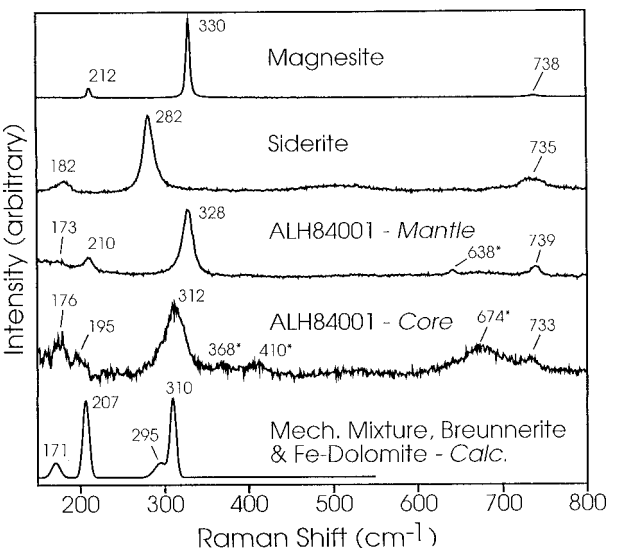

Figure 3. Confocal micro-Raman spectra (lattice-mode spectral region) of the irregular carbonate globule from ALH84001,6 obtained with 1800 gr/mm grating at 3 cm^{-1} resolution. Meteorite carbonate spectra (third and fourth curves from top) compared to those of terrestrial $MgCO_3$ (upper curve), $FeCO_3$ (second curve from top) and a calculated spectrum (lower curve) representing the expected results for a mechanical mixture of ferroan magnesite and ferroan dolomite. Curve labeled "mantle" taken between two concentric bands of opaque inclusions (point no. 1 of Fig. 1); curve labeled "core" obtained from CaFe-carbonate-enriched central region (just within inner opaque ring, point no. 2 of Fig. 1). The meteorite carbonate spectra (third and fourth curves from the top) have been corrected for fluorescence by subtraction of a sloping baseline. See text for further discussion. Peaks marked with asterisks are from either mounting epoxy (638 cm^{-1}) or included magnetite.

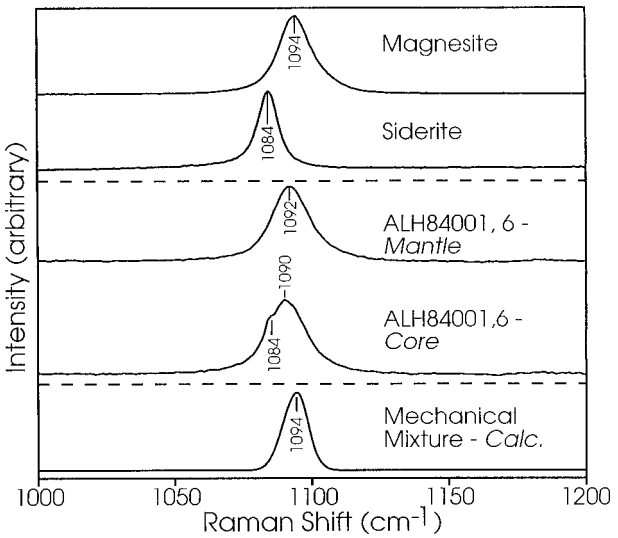

FIGURE 4. Confocal micro-Raman spectra (C-O stretch spectral region) of the irregular carbonate globule from ALH84001,6 shown in Figure 1. Meteorite carbonate spectra compared to the measured spectra of terrestrial magnesite, siderite and a calculated spectrum representing the expected results for a mechanical mixture of breunnerite and ferroan dolomite. Curve designations are same as in Figure 3. The spectra of Figure 4 were not obtained simultaneously with those of Figure 3, but an attempt was made to re-visit the same spots (marked in Fig. 1) as closely as possible.

The chemical zonation trend of ALH84001 carbonates crosses a miscibility gap and Valley et al. (1997) have thus speculated that these carbonates may exhibit sub-micrometer phase exsolution characteristic of low temperature growth. To address this question, we compared the observed ALH84001 carbonate Raman spectra with calculated Raman spectra of simple mechanical mixtures of breunnerite and ferroan dolomite having the same bulk composition (specifically $Ca_{0.08}Fe_{0.30}Mg_{0.62}CO_3$) as that estimated for the carbonate at point "2" of Figure 1. In this calculation, we used (1) the carbonate end-member Raman band positions of magnesite, siderite, dolomite, and ankerite (Herman et al. 1987); (2) our own measurements of spectral band width of magnesite, dolomite, and siderite; (3) an assumption of linear change of band position and band width with composition in each solid solution series (breunnerite and ferroan dolomite); (4) Gaussian band shapes; (5) an assumption of co-existing phase compositions respectively along the $MgCO_3$-$FeCO_3$ and $CaMg(CO_3)_2$-$CaFe(CO_3)_2$ joins; and (6) no Fe/Mg partitioning between the two hypothetical carbonate phases. The latter two assumptions are roughly consistent with analyses of terrestrial carbonate phase assemblages (Essene 1983). These simulated spectra exhibit fully or partially resolved "doublets" in the lattice-mode region (Fig. 3) but only show slight broadening or development of asymmetry of other bands, as compared to Raman spectra of single-phase carbonates (Fig. 4). The ALH84001 carbonates—especially those of the CaFe-enriched inner regions—appear to exhibit similar splitting (i.e., the apparent presence of two bands below 200 cm^{-1}, Fig. 3), shoulder development (i.e., 1084 cm^{-1} shoulder on 1090 cm^{-1} band, Fig. 4), and asymmetry (312 cm^{-1} band, Fig. 3). These features suggest that the ALH84001 carbonates are either multiphase or compositionally heterogeneous on a submicroscopic scale. However, the greater widths and variability of the ALH84001 carbonate Raman bands than those in the calculated spectra suggest that the compositional heterogeneity is more complex than simple two-phase unmixing. Although a range of compositions is suggested by these data, the occasional split bands and shoulders (Figs. 3 and 4) suggest the presence of some proportion of a separate Ca-enriched carbonate (dolomite or possibly calcite) in carbonates whose bulk compositions are close to the $MgCO_3$-$FeCO_3$ join.

Raman band broadening has been observed in single-phase synthetic and biogenic magnesian calcites (Bischoff et al. 1985) as a result of both cationic mixing disorder and anionic positional disorder (tilting of CO_3^{2-} ions out of the crystallographic basal plane). The lattice mode bandwidths of biogenic magnesian calcites are greater and more variable than those of synthetic carbonates of similar composition because of greater positional disorder (Bischoff et al. 1985). As in the Raman spectra of biogenic carbonates, the carbonate lattice mode vibrations in ALH84001 are similarly broad and variable (Fig. 3). However, there are currently no systematic studies of the variation of Raman band positions and widths as a function of composition for Fe-bearing carbonate solid solutions like those in ALH84001. As discussed above, part of the band broadening may be the result of complex sub-microscopic compositional heterogeneity. Further experimental studies are thus required to test whether the general Raman band broadening in ALH84001 carbonates is the result of biogenic origin, cation disorder, quenching from high temperatures, partial sub-solidus unmixing, or some other cause.

Silica

The Raman spectrum of the silica grain (Fig. 5a) shows broad features indicating it is predominantly amorphous. The weak, sharp peak at 462 cm^{-1} is attributable to a minor proportion (1–5%) of crystalline quartz; the band at 400 cm^{-1} may result from a trace amount of tridymite. There is no evidence of the diagnostic Raman bands of other crystalline silica polymorphs (stishovite, 753 cm^{-1}; cristobalite, 416 cm^{-1}; coesite, 521 cm^{-1}).

The Raman spectrum of the silica grain is similar to that of the thermal glass (Fig. 5) in the low-wavenumber region (Sharma et al. 1981) but exhibits a distinct shift of the mid-frequency band to greater wavenumbers (from 797 to 814 cm^{-1}). The high-wavenumber features are too weak to discern in this microscopic sample; the small 1100 cm^{-1} feature is probably spectral contamination from the glass slide. Raman spectra of laboratory shocked quartz revealed significant residual crystallinity (strong, sharp Raman peaks) up to peak shock pressures of 31 GPa (McMillan et al. 1992) but a rapid change to total amorphization at peak pressures near 32 GPa (Champagnon et al. 1996). Within the uncertainties of interpreting peak shock pressures (Sharp et al. 1997; Chen et al. 1996), the largely glassy character of the ALH84001 silica grain spectrum thus suggests peak pres-

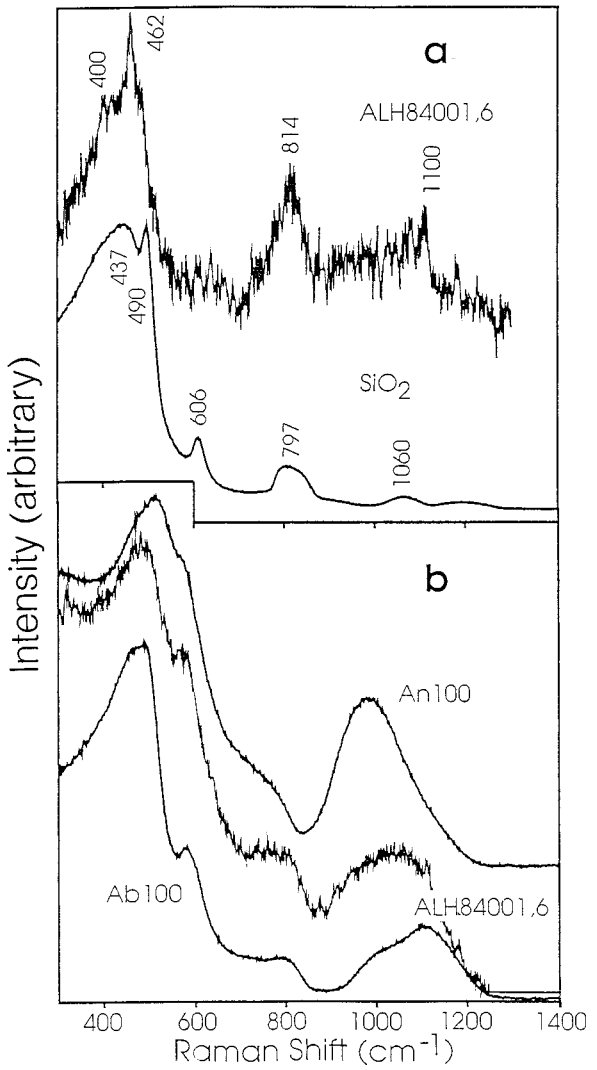

FIGURE 5. Confocal micro-Raman spectra of (**a**) silica in ALH84001,6 (Fig. 2a) and (**b**) vitreous plagioclase in ALH84001,146 compared to those of synthetic thermal glasses. Labels Ab100 and An100 denote synthetic albite-composition and anorthite-composition thermal glasses, respectively.

sures at least 32 GPa. Because of the residual crystalline peaks, it appears that this particular silica grain was not melted. If the silica was, in fact, shock melted, much higher peak pressures are within reason. In fact, other silica grains in the rock do appear to have been melted and mobilized (Scott et al. 1997).

Amorphous feldspar

Feldspathic glasses in ALH94001, as in most Martian meteorites are optically isotropic due to shock. Previous authors have generally assumed that these phases, often called maskelynite, formed by solid-state processes (Stöffler 1986). However, in ALH84001, some grains appear to have flowed into fractures as melts, contain rare vesicles, and show significant deviations from plagioclase composition (Scott et al. 1997). Raman studies are needed to understand the origin of the feldspathic phases and to constrain their shock history.

Shock amorphization effects in feldspar are thought to be similar to those of silica because of the similar tectosilicate structures in both crystalline and glassy states (Richet and Gillet 1997). The existing Raman data on feldspars shock-amorphized in the laboratory at peak shock pressures up to 50 GPa (Velde et al. 1989) suggest that the spectra are highly variable and slightly different from compositionally similar thermal glasses. Heymann and Hörz (1990) noted progressive weakening and ultimate disappearance of crystalline-related Raman and XRD peaks in experimentally shocked oligoclase and microcline near 30 GPa. Progressive band broadening and loss of spectral detail in IR spectra of shocked feldspar have also been interpreted in terms of progressive increase in glassy fraction with increasing shock pressure (Velde et al. 1987). Static amorphization of anorthite was first noted from IR spectroscopy of material recovered from high-pressure diamond anvil studies (Williams and Jeanloz 1989). More recently, detailed Raman and synchrotron XRD study of static compression and amorphization of anorthite up to 30 GPa (Daniel et al. 1997) has shown the dependence of amorphization pressure upon deviatoric stress, and the important role of decompression history on the degree of amorphization in recovered pressure-quenched samples. Specifically, it was found that, although the Raman spectrum of recovered pressure-amorphized anorthite is similar to that of thermal glass, there is an increase in the relative intensity of the 580 cm^{-1} shoulder, suggesting a non-reversible increase in the proportion of three-member aluminosilicate rings (Daniel et al. 1997).

The intermediate character of the ALH84001 vitreous feldspar spectrum between those of the synthetic end-member glasses (Fig. 5b) is consistent with its average composition of approximately An_{33} (Mittlefehldt 1994). Raman spectra of several other vitreous feldspar grains do not show any significant deviations from the spectrum illustrated in Figure 5b. The lack of spectral evidence of densification, as would be characterized by increase in intensity (Daniel et al. 1997) of the 580 cm^{-1} shoulder, and the similarity of spectra from multiple grains, in contrast to significant variability (Velde and Boyer 1985; Velde et al. 1994) observed in Raman spectra of shocked feldspars from a single sample or thin section, together suggest that this glass achieved its final structural configuration from quenching of a melt at a lower pressure than that required for solid-state amorphization. Because there is clear petrographic evidence that the feldspar was amorphized by shock (Scott et al. 1997), the spectroscopic results thus suggest that this material was quenched from a high-temperature, low-pressure (less than several GPa) liquid associated with residual heat from the shock event. This shock event was of sufficient intensity (ca 50 GPa) to completely melt or amorphize pre-existing crystalline feldspar (Stöffler 1984). The existence of feldspar melt is consistent with the observation of reaction between feldspar and carbonates at their interface (Brearley 1998).

Phosphates

In phosphates, water (as well as fluorine and chlorine) behaves as a compatible trace component and these minerals are

therefore very sensitive indicators of water availability (Dowty 1977). The identification of the Mg-bearing phosphate phase as merrillite (β-Ca-phosphate structure) is made by comparing its Raman and IR-reflectance spectra (Fig. 6) to those of synthetic phosphates having the β-$Ca_3(PO_4)_2$ structure (Mooney et al. 1968; de Aza et al. 1997). Petrographic study indicates that most of the phosphate in this rock is, in fact, merrillite, and that the two phases exhibit a replacement relationship. Importantly, the structure of anhydrous merrillite (known from the Moon and chondritic meteorites) is different from that of whitlockite (terrestrial), which preferentially incorporates water (Dowty 1977).

The bands between 947 and 974 cm^{-1}, which are strong in the Raman spectra and of intermediate intensity in the IR originate from the ν_1 symmetric stretching mode of PO_4^{3-} ions (O'Shea et al. 1974). Bands in the 1000–1150 cm^{-1} region of all spectra (Fig. 6), which exhibit opposite relative intensities, result from antisymmetric ν_3 vibrations (Mooney et al. 1968). In the 1400 and 1700 cm^{-1} region of IR reflectance spectra of these phosphates (not shown in Fig. 6) no evidence was found for the presence of OH or molecular H_2O. The Raman spectrum of merrillite shows no evidence of the P-OH stretching band that occurs at 923 cm^{-1} in spectra of terrestrial whitlockite (Jolliff et al. 1996). Also absent, from the Raman spectrum of ALH84001 apatite is any indication of the OH^- librational band at 655 cm^{-1} characteristic of hydroxyapatite (O'Shea et al. 1974). Together, these data indicate either that the ALH84001 phosphates formed in the absence of water or else were degassed during shock. Although nothing is known about possible shock amorphization of phosphates, static amorphization occurs at pressures near 10 GPa (Vaidya et al. 1997), somewhat lower than for feldspars. Truncations of phosphates at fracture zones indicate that these minerals predate shock events, yet coarse-grained apatite and merrillite occur next to shock-produced plagioclase glass (Fig. 3b). The possible explanations are either (1) that the shock experienced by ALH84001 did not produce diaplectic phosphate glass, (2) phosphates devitrify more readily than feldspars, or (3) phosphates crystallized from a phosphate shock melt, whose formation may have been aided, in the initial stages, by water of dehydration from precursor hydroxyapatite. Some apparent re-mobilization of phosphate adjacent to pyroxene (Fig. 2b) favors the latter hypothesis.

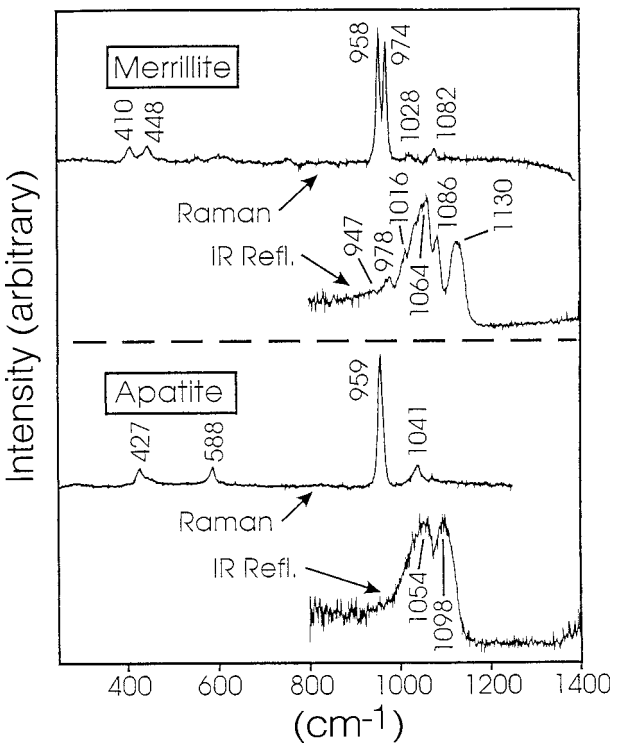

FIGURE 6. Partial confocal micro-Raman and FT-IR reflectance spectra of phosphates (merrillite and apatite) measured in the ALH84001,6 thin section (Fig. 2b).

CONCLUSIONS

Confocal micro-Raman spectroscopy provides valuable complimentary structural information with a few micrometers resolution on both crystalline and glassy phases in Martian meteorite ALH84001. The observed general Raman band broadening in ALH84001 carbonate spectra indicates complex submicroscopic compositional heterogeneity and possibly structural disorder. The information from amorphous silica and plagioclase clearly indicates that carbonate and other minor phases in ALH84001 have experienced complex thermal and shock histories, including possible post-shock annealing and melting. Future controlled laboratory studies on structural disorder and its Raman spectral expression in Fe-Mg-Ca carbonates and on shock metamorphism of phosphates are needed to better constrain this complex history. This structural evidence must be recognized in the interpretation of chemical and isotopic data and in any search for biogenic markers.

ACKNOWLEDGMENTS

The authors thank Alian Wang, Washington University, St. Louis, and Allan H. Trieman, Lunar and Planetary Institute, Houston, for their constructive comments on an earlier version of this manuscript. The manuscript has also benefited with. Anne Hofmeister's editorial comments. This work was supported, in part, by NSF grant no. OPP-9714012 (E.R.D. Scott, Principal Investigator) and NASA grant NAGW 3281 (K. Keil, Principal Investigator). This is SOEST contribution no. 4839 and HIGP contribution no. 1062.

REFERENCES CITED

Bischoff, W.D., Sharma, S.K., and Mackenzie, F.T. (1985) Carbonate ion disorder in synthetic and biogenic magnesian calcites: a Raman spectral study. American Mineralogist, 70, 581–589.

Boctor, N.Z., Wang, J., Alexander, C.O.A., Hauri, E., Bertka, C.M., Fei, Y., and Humayun, M. (1998) Petrology and hydrogen and sulfur isotope studies of mineral phases in Martian meteorite ALH 84001. In Lunar and Planetary Science 29, Abstract no. 1787. Lunar and Planetary Institute, Houston (CD-ROM).

Bradley, J.P., Harvey, R.P., and McSween, H.Y. Jr. (1996) Magnetite whiskers and platelets in the ALH84001 Martian meteorite: evidence of vapor phase growth. Geochimica et Cosmochimica Acta, 60, 5149–5155.

Brearley, A.J. (1998) Microstructures of feldspathic glass in ALH84001 and evidence for post carbonate formation shock melting. In: Lunar and Planetary Science 29, Abstract no. 1452. Lunar and Planetary Institute, Houston (CD-ROM).

Champagnon, B., Panczer, G., Chemarin, C., and Humbert-Labeaumaz, B. (1996) Raman study of quartz amorphization by shock pressure. Journal of Non-Crystalline Solids, 196, 221–226.

Chen, M., Sharp, T.G., El Goresy, A., Wopenka, B., and Xie, X (1996) The majorite-pyrope + magnesiowüstite assemblage: constraints on the history of shock veins in chondrites. Science, 271, 1570–1573.

Daniel, I., Gillet, P., McMillan, P.F., Wolf, G., and Verhelst, M.A. (1997) High-pressure behavior of anorthite: compression and amorphization. Journal of Geophysical Research, 102, 10313–10325.

de Aza, P.N., Santos, C., Pazo, A., de Aza, S., Cusco, R., and Artús, L. (1997) Vibrational properties of calcium phosphate compounds: 1. Raman spectrum of beta-tricalcium phosphate. Chemistry of Materials, 9, 912–915.

Dowty, E. (1977) Phosphate in Angra Dos Reis: structure and composition of the $Ca_3(PO_4)_2$ minerals. Earth and Planetary Science Letters, 35, 347–351.

El Goresy, A., Wopenka, B., Chen, M., and Kurat, G. (1997) The saga of maskelynite in Shergotty (abstract) Meteoritics and Planetary Science, 32, A38–A39.

Essene, E.J. (1983) Carbonates: mineralogy and chemistry. In Mineralogical Society of America Reviews in Mineralogy, 11, 76–96.

Gleason, J.D., Kring, D.A., Hill, D.H., and Boynton, W.V. (1997) Petrography and bulk chemistry of Martian orthopyroxenite ALH84001: implications for the origin of secondary carbonates. Geochimica et Cosmochimica Acta, 61, 3503–3512.

Harvey, R.P. and McSween, H.Y. Jr. (1996) A possible high-temperature origin for the carbonates in the martian meteorite ALH84001. Nature, 382, 49–51.

Herman, R.G., Bogdan, C.E., Sommer, A.J., and Simpson, D.R. (1987) Discrimination among carbonate minerals by Raman spectroscopy using the laser microprobe. Applied Spectroscopy, 41, 437–440.

Heymann, D. and Hörz, F. (1990) Raman spectroscopy and X-ray diffractometer studies of experimentally produced diaplectic feldspar glass. Physics and Chemistry of Minerals, 17, 38–44.

Jolliff, B.L., Freeman, J.J., and Wopenka, B. (1996) Structural comparison of lunar, terrestrial, and synthetic whitlockite using laser Raman microprobe spectroscopy. Abstracts of the Lunar and Planetary Science Conference, XXVII, 613–614.

Kring, D.A., Timothy, D., Gleason, J.D., and Grier, J.A. (1998) Formation and relative ages of maskelynite and carbonate in AlH84001. Geochimica et Cosmochimica Acta, 62, 2155–2166.

Leshin, L.A., Harvey, R.P., McCoy, T.J., and McKeegan, K.D. (1996) Water in apatite from Shergottite QUE94201: abundance and D/H. Meteoritics and Planetary Science, 31, A79–A80.

Leshin, L.A., McKeegan, K.D., Carpenter, P.K., and Harvey, R.P. (1998) Oxygen isotopic constraints on the genesis of carbonates from Martian meteorite ALH84001. Geochimica et Cosmochimica Acta, 62, 3–13.

McKay, D.S., Gibson, E.K. Jr., Thomas-Keptra, K.L.H., Vali, H., Romanek, C.S., Clemett, S.J., Chiller, X.D.F., Maechling, C.R., and Zare, R.N. (1996) Search for past life on Mars: possible relic biogenic activity in Martian meteorite ALH84001. Science, 273, 924–930.

McMillan, P.F., Wolf, G.H., and Lambert, P. (1992) A Raman spectroscopic study of shocked single crystalline quartz. Physics and Chemistry of Minerals, 19, 71–79.

Mittlefehldt, D.W. (1994) ALH84001, a cumulate orthopyroxenite member of the martian meteorite clan. Meteoritics, 29, 214–221.

Mooney, R.W., Toma, S.Z., Goldsmith, R.L., and Butler, K.H. (1968) Normal vibrations of the PO_4^{3-} ion, site symmetry, C_{3v}, in $Sr_3(PO_4)_2$ and $Ba_3(PO_4)_2$. Journal of Inorganic and Nuclear Chemistry, 30, 1669–1675.

O'Shea, D.C., Bartlett, M.L., and Young, R.A. (1974) Compositional analysis of apatites with laser-Raman spectroscopy: (OH,F,Cl)Apatites. Archives of Oral Biology, 19, 995–1006.

Richet, P. and Gillet, P. (1997) Pressure-induced amorphization of minerals: a review. European Journal of Mineralogy, 9, 907–933.

Romanek, C.S., Grady, M.M., Wright, I.P., Mittlefehldt, D.W., Socki, R.A., Pillinger, C.T., and Gibson, E.K., Jr. (1994) Record of fluid-rock interactions on Mars from the meteorite ALH84001. Nature, 372, 655–657.

Rubin, A.E. (1997) Mineralogy of meteorite groups: an update. Meteoritics and Planetary Science, 32, 733–734.

Saxton, J.M., Lyon, I.C., and Turner, G. (1998) Correlated chemical and isotopic zoning in carbonates in martian meteorite ALH84001. Earth and Planetary Science Letters 160, 811–822.

Scott, E.R.D., Yamaguchi, A., and Krot, A.N. (1997) Petrological evidence for shock melting of carbonates in the Martian meteorite ALH84001. Nature, 387, 377–379.

Sharma, S.K. (1989) Applications of advanced Raman spectroscopic techniques in earth sciences. Vibrational Spectra and Structure, 17B, 513–568.

Sharma, S.K., Mammone, J.F., and Nicol, M.F. (1981) Raman investigation of ring configurations in vitreous silica. Nature, 292, 140–141.

Sharma, S.K., Wang, Z., and van der Laan, S. (1996) Raman spectroscopy of oxide glasses at high pressure and high temperature. Journal of Raman Spectroscopy, 27, 739–746.

Sharp, T.G., Lingemann, C.M., Dupas, C., and Stöffler, D. (1997) Natural occurrence of $MgSiO_3$-ilmenite and evidence for $MgSiO_3$-perovskite in a shocked L chondrite. Science, 277, 352–355.

Stöffler, D. (1984) Glasses formed by hypervelocity impact. Journal of Non-Crystalline Solids, 67, 465–502.

Stöffler, D. and Langenhorst, F. (1994) Shock metamorphism of quartz in nature and experiment: I. Basic observation and theory. Meteoritics, 29, 155–181.

Stöffler, D., Ostertag, R., Jammes, C., Pfannschmidt, G., Sen Gupta, P.R., Simonm S.B., Papike, J.J., and Beauchamp, R.H. (1986) Shock metamorphism and petrography of the Shergotty achondrite. Geochimica et Cosmochimica Acta, 50, 889–903.

Treiman, A.H. (1997) Chemical Disequilibrium in carbonate minerals of Martian meteorite ALH84001: inconsistent with high formation temperature. Proceedings of the Lunar and Planetary Science Conference, 28, 1445–1446.

Vaidya, S.N., Sughandhi, V., and Roy, A.P. (1997) Pressure induced crystalline to amorphous transition in calcium phosphates. Advances in High Pressure Research Condensed Matter, 139–145.

Valley, J.W. et al. (1997) Low temperature carbonate concretions in the Martian meteorite ALH84001: evidence from stable isotopes and mineralogy. Science, 275, 1633–1638.

Velde, B. and Boyer, H. (1985) Raman microprobe spectra of naturally shocked microcline feldspars. Journal of Geophysical Research, 90, 3675–3682.

Velde, B., Syono, Y., Couty, R., and Kikuchi, M. (1987) High pressure infrared spectra of diaplectic anorthite glass. Physics and Chemistry of Minerals, 14, 345–349.

Velde, B., Syono, Y., Kikuchi, M., and Boyer, H. (1989) Raman microprobe study of synthetic diaplectic plagioclase feldspars. Physics and Chemistry of Minerals, 16, 436–441.

Wang, A., Joliff, B.L., and Haskin, L.A. (1998) Raman spectroscopic characterization of Martian meteorite Zagami. In Lunar and Planetary Science 29, Abstract no. 1523. Lunar and Planetary Institute, Houston (CD-ROM).

White, W.B. (1974) The carbonate minerals. In: V.C. Farmer (Ed.), The Infra-red Spectra of Minerals, Mineralogical Society, Monograph 4, Chapter 12, p. 227–284. London.

Williams, Q. and Jeanloz, R. (1989) Static amorphization of anorthite at 300 K and comparison with diaplectic glass. Nature, 338, 413–415.

Wopenka, B., Chen, M., and El Goresy, A. (1996) Microsampling Raman spectroscopy: a nifty technique for the unambiguous in situ identification of micrometer-sized shock-induced polymorphs in L6 chondrites (abstract). Meteoritics, 31, A155–A156.

MANUSCRIPT RECEIVED AUGUST 3, 1998
MANUSCRIPT ACCEPTED JUNE 1, 1999
PAPER HANDLED BY ANNE M. HOFMEISTER